A Scaled-Correlation based approach for defining and analyzing functional networks

Samuel Dolean[1], Mihaela Dînșoreanu[1], Raul Cristian Mureșan[2]
Attila Geiszt[1], Rodica Potolea[1], and Ioana Țincaș[2]

[1] Technical University of Cluj-Napoca, Department of Computer Science, Cluj-Napoca, Romania
samm.dlln@yahoo.co.uk, Mihaela.Dinsoreanu@cs.utcluj.ro,
attila.geiszt@gmail.com, Rodica.Potolea@cs.utcluj.ro
[2] Transylvanian Institute of Neuroscience, Cluj-Napoca, Romania
muresan@tins.ro, tincas@tins.ro

Abstract. Many natural systems can be described as networks of interacting elements, forming a graph of interactions. This is the case for climate models, coupled chemical systems, computer or social networks, or the brain. For many of these cases, dynamical networks emerge whose structure changes in time. Estimating the structure of such networks from the time series that describe the activity of their nodes is a serious challenge. Here, we devise a new method that is based on the Scaled Correlation function to estimate interactions between nodes that occur on fast timescales. We apply the method on EEG measurements from human volunteers to evaluate neuronal functional connectivity associated with a visual perception task. We compare the statistics of networks extracted with the new method with those that are extracted using traditional techniques, like the Pearson correlation coefficient or the cross-correlation function. Results indicate that the new method is superior in identifying networks whose structure correlates to the cognitive processes engaged during visual perception. The method is general enough to be applied on any data that describes dynamical interactions evolving on multiple timescales, as is the case in climate modeling, chemical networks, or complex biological systems.

Keywords: EEG, functional brain networks, metrics, Cross-Correlation, Scaled-Correlation, Pearson correlation coefficient, directed weighted network

1 Introduction

Network science [1] has become a major research field in the past decade, relying heavily on computational methods to extract and characterize networks from complex data. A wide variety of systems can be described as connected graphs, from computer networks, social interaction patterns, disease spreading models, to biological networks. Networks can even be found in the legal system [2] and tourism [3]. Importantly, many of these networks are dynamical, in

the sense that individual nodes exhibit a time-dependent activity that shapes interaction patterns with the other nodes. Such is the case of complex brain networks [4], whereby different brain regions connect and disconnect all the time as a function of cognitive processing, thus yielding functional networks whose structure evolves in time. Similarly, in climate modeling one constructs networks from modeled space-time series [5], yielding complex dynamical graphs. A large effort has been dedicated to characterizing complex networks but less attention has been paid to how these networks are defined and extracted from the data, although this is a critical step. For dynamical networks, each node has an associated activity that can be described as a time series. To evaluate if two nodes are functionally connected, the traditional procedure is to use the pairwise Pearson correlation coefficient [6] or the cross-correlation function [7]. Arguably, both of these methods are sub optimal because they either do not consider the full temporal structure of the data (e.g., delays), or cannot distinguish faster from slower interactions, respectively. Here we develop a novel method to extract networks from complex time series using the Scaled Correlation function (SCF) that can estimate interactions on the fast timescales by means of restricted sampling [8]. We apply this method on a hard test case, defining and characterizing functional brain networks from high-density EEG signals recorded in humans during a demanding visual task. The challenge is to determine if statistics of networks extracted using SCF correlate better to the cognitive task that participants have to solve than those extracted with traditional techniques. To this end, we focused on three different types of networks: Pearson Coefficient Weighted Networks (PCWN), Cross Correlation Weighted Networks (CCWN), and Scaled Correlation Weighted Networks (SCWN) and for each we evaluated network theory metrics.

2 Related Work

Three types of neural connectivity are considered in the literature [9]: structural, functional, and effective. Structural connectivity pertains to the physical, anatomical connections between brain areas and is considered to be fixed on a short term. By contrast, functional connectivity expresses sub-graphs of the anatomical network that are transiently coupled, depending on the activity of the nodes [10]. Effective connectivity constrains the graph further by considering only those interactions that mediate the reciprocal influence of brain areas [9].

Here we focused on functional connectivity, as it is more widely used and easier to estimate. The basic theoretical framework for graph/network analysis of functional connectivity is given in [4], with more advanced metrics being defined in [11]. The community and hub structure dynamic was studied in [12], that concluding that increasing the cognitive task difficulty leads to lower modularity, fewer provincial hubs, and more connector hubs. The relevance of the network size was studied in [13], showing that different metrics depend on it (i.e. clustering coefficient, modularity, efficiency, economic efficiency and assortativity). The conclusion was that efficiency, assortativity were higher and modularity

was lower on large networks compared to smaller networks, even though their density was the same.

Functional brain connectivity is usually estimated by computing pairwise correlations between activities of different neural populations. The most popular measure of correlation is the Pearson Correlation coefficient (PCC). Also, a related approach was presented in [14] by computing partial correlations between pairs of signals. Partial correlation consists of calculating PCC but augmenting this coefficient in order to eliminate the influence of potential third-party signals. One of the most important conclusions is that using first grade partial correlations the distribution of values are centered around zero whereas non-partial correlations (simple PCC) were spread along the [0,1] interval.

PCC as well as its partial counterpart ignore the multiple timescales present in neural signals. For example, fast oscillations in the gamma band (30-80 Hz) are expressed in relation to a plethora of cognitive and perceptual processes but traditional measures, like the PCC, cannot selectively evaluate the fast-timescale correlations induced by such oscillations. By contrast, we have developed a measure called Scaled Correlation [8], which isolates correlations expressed on fast timescales by using restricted sampling.

Here, we analyzed EEG data recorded from human volunteers performing a visual recognition task. Participants had to identify objects from images of stimuli containing deformed grids / lattices of dots (see the "Dots" method for a reference) . The varying deformation of these lattices made recognition easier or harder. Our objective was to evaluate how functional brain connectivity changes when the subjects engage in the perceptual task, compared to the "baseline" condition (i.e., before the stimulus was shown on the screen). We wanted to determine which measure of connectivity is able to more efficiently reveal the reorganization of functional networks during perceptual engagement.

3 Relevant Concepts

A **participant** is defined as one of the individuals that took part in the experiment, and for which specific data was recorded.

A **trial** is a part of an experiment, time-wise. An experiment is divided into several trials (in our case, 210 trials), and each trial contains some events. In this experiment the trials have different lengths, as the participants were free to explore. An **event** consists of a specific time instant relative to the beginning of the trial and a unique code which has significance for the experiment.

A **correlogram** is the result of a correlation function [8] applied on two signals. As the correlogram is an array of values, the **peak** of a correlogram is the maximum absolute value along all values. The **lag** is the position where the **peak** was found in the correlogram.

The **stimulus** refers to the moment when the picture is displayed on screen. We call **baseline** the moment right before the stimulus appears.

An **area** is one of the brain regions (occipital, frontal, parietal, left temporal and right temporal). In our case it is represented by a group of electrodes (whose coordinates are given by the headset used in experiment).

4 Identification of functional networks

For each participant and for each trial, we do the following steps: first, using the recorded signals, we construct graphs using different correlations to estimate the functional connectivity, and then we apply metrics from complex network theory on these graphs in order to investigate the relevance of the metrics and to analyze properties of the network (Fig. 1). These steps are further explained in the following paragraphs.

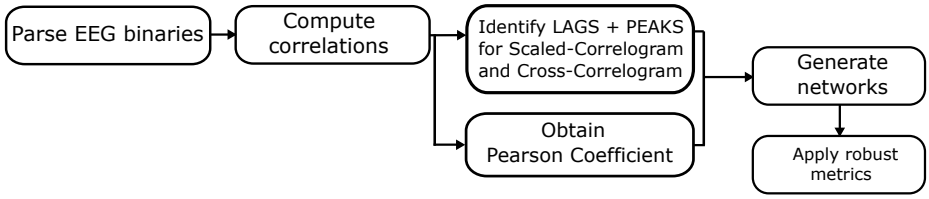

Fig. 1. Lags, Peaks and Pearson weighted networks approach used

The first phase consists of parsing the EEG signals recorded from the participants. Based on these signals we compute various correlation functions. We use three types of functions: Cross-Correlation (CCF), Scaled-Correlation (SCF) [8] and Pearson Correlation Coefficient (PCC). Based on the resulted cross/scaled-correlogram (in case of CCF and SCF) we identify lags and peaks. In the case of PCC we simply use it without further processing. The decision of using PCC is based on its frequent use in literature. However this coefficient fails to represent the timing relation (i.e., delay) between signals, its value representing only the instantaneous correlation at lag zero. In contrast, SCF and CCF slides the signals in time enabling to identify delays that indicate potential causality relations between signals.

In the next phase, we create five kinds of graphs, referred by us as the PCCWN (Peaks Cross Correlation weighted Network), LCCWN (Lags Cross Correlation weighted Network), PSCWN (Peaks Scaled Correlation weighted Network), LSCWN (Lags Scaled Correlation weighted Network) and the PCWN (Pearson Coefficient weighted Network). All these graphs have 128 nodes, corresponding to the 128 EEG channels.

The *PCWN* is an undirected weighted graph which has the absolute values of the Pearson correlation coefficient (samples version) as weights between any two nodes. The Pearson correlation coefficient shows how linearly correlated two signals are varying from: 1 - the signals are perfectly linearly correlated, to -1 - they are perfectly anti-correlated.

The *PCCWN* and *PSCWN* are directed graphs having edges with weight defined as the the absolute value of the largest peak from the cross/scaled-correlogram [8], respectively. The *LSCWN* and *LCCWN* are directed graphs as well but the weights of the edges are the absolute values of the lags of the peaks identified previously. The absolute peak value is the strongest correlation value at time t. As we mentioned a negative correlation indicates the anti-correlation which is perfectly fine because it means that most probably the two signals come from opposite electrode sites. The lag of this peak indicates the delay of information transfer hence the bigger the distance from 0, the higher delay it is obtained no matter if it is negative or positive. In the case of the LSCWN, LCCWN, PSCWN, and PCCWN the direction of the edge is defined by the lag sign. Considering channels A and B, a positive lag shows B leading A while a negative lag shows A leading B. When the lag is 0, we consider that the channels are instantaneously correlated and we assign two bidirectional edges (from A to B and from B to A). For channels with the same index (diagonal) the value in the matrix is zero.

For the window of the CCF we have chosen a window of +/-100 ms, which has the effect of focusing on small delays. For the SCF we applied a scale window segment of 25 ms to keep only correlations between components that have a frequency greater than 40 Hz. We have chosen to use Pearson-based and Scaled-Correlation based networks to compare results obtained with the traditional method with those which extract only the fast correlations of the signals, considered to be important for conscious visual perception [15]. However we decided to go for Cross-Correlation as well because we want to understand if considering the temporal structure (delays) of signals brings additional benefits compared to the PCC. The CCF is used without any normalization.

For each network we decided to reduce its density (keeping only 50% of the edges with the strongest weights). The motivation behind the thresholding is that we also considered the reduction of potential noises that may alter the correlation values [16]. Another reason for density reduction is because of the extremely high density of PCWN which is a complete graph, hence the metrics would lead to improper results. Furthermore, we chose to take the absolute value for edge weights because negative edge weights are affecting graph metrics (i.e., Average Path Length) while the absolute value still captures the information about the correlation strength.

For the second analysis (per areas) we didn't consider a 50% density reduction since we are interested in raw values of the peaks and lags as they were initially computed. In order to be consistent with the previous strategy for the metrics, we kept the absolute values too in this new analysis.

The following measures have been applied: average path length (APL) [17][18], global clustering coefficient (GCC) [19], betweenness centrality (BC) and closeness centrality (CC) [17]. For each measure we study the modifications of the global network statistics by comparing CC, SC and PCC.

APL has been considered on the obtained graphs and the computation was done by using Dijkstra shortest path algorithm [20]. In order to achieve the

average path length based on the shortest paths between each two nodes, the following formula has been applied:

$$apl_{G_{weighted}} = \frac{1}{N(N-1)} \sum p_{i,j}, i \neq j \quad (1)$$

where $p_{i,j}$ is the shortest path between node i and j and N is the total number of nodes. Because this metric is a distance based metric we applied it only on the lags network. However in the case of the Pearson network, we consider stronger connections as closer connections by inversing the edge weights in the computation of the shortest path.

5 Experimental results

5.1 Data description

Electroencephalography (EEG) data was recorded from 10 healthy human volunteers performing a visual recognition task. A high-density Biosemi ActiveTwo machine, with 128 channels was used to record scalp potentials with a sampling rate of 1024 samples/s. The experimental protocol followed the one described in [21], with several important modifications. Participants were shown visual stimuli that represented shapes of 30 objects through a lattice of dots that was distorted to capture object contours (see the "Dots method" in [21]). The experiment was organized in 7 successive blocks of 30 stimuli, each block being characterized by a different level of distortion. The first block contained no distortion of the lattice, and thereby no information about the object, whereas the seventh block contained the maximal distortion, enabling effortless recognition of the objects. Blocks were shown in ascending order of distortion, thus rendering objects increasingly more visible in successive blocks. This yielded a total of 210 trials (30 stimuli / block x 7 blocks). Compared to our previous study [21], here we used only a subset of 30 stimuli that were validated in a pilot experiment – only objects that provided unambiguous recognition were included. Also, data was recorded from 10 novel participants with an "ascending" protocol only, i.e. increasing visibility in successive blocks. Data from all the 10 subjects was analyzed.

Each individual trial consisted of several periods that were delineated by using TTL pulses on an 8-bit line delivered to the EEG machine by a National Instruments PCI-6503 board controlled by the stimulation computer (see Fig. 2). Trial start was signaled by an event code (trigger) 128 and was followed by the presentation of a red fixation dot in the center of the screen, which subjects had to watch for 1-1.5 s. A new trigger value of 150 was then followed by a white, full screen mask kept for 500 ms. Then, a 129 trigger code was issued simultaneously with the presentation of the dot stimulus on screen. Subjects were free to visually explore the stimulus and then had to press one of three keys, signaling that they i) have seen the object and can name it (trigger code = 1), or ii) have seen something but are uncertain about the object it represents

(trigger code = 2), or iii) haven't seen any object (trigger code = 3). Each baseline (segment between triggers 150 and 129) and stimulus (segment between trigger 129 and trigger 1,2, or 3) periods of a trial in the raw EEG data was represented as a matrix of floating-point values, where each row corresponded to a channel (128 rows) and columns corresponded to the samples during the baseline and stimulus period, respectively (see Fig. 2). Different participants had a different number of trials for each response type: e.g., the first participant had 63 seen trials, 53 uncertain trials and 94 trials where he recognized nothing. Other participants had different numbers of trials for each response type. Once all trials are parsed and gathered from the raw data for each response category, we computed the CCF, SCF and PCC for each pair of channels. The networks we obtained were represented as square (128 x 128) adjacency matrices, where we ignored the primary diagonal (self-connectivity of nodes). Matrices for PCCWN (based on CCF) and PSCWN (based on SCF) contained, for each row-column pair a value between [-1,1] representing the value of the largest peak in the correlogram. In the case of LCCWN and LSCWN, this value was taken to be the lag where the peak was positioned in the correlogram. Finally, for PCWN (Pearson correlation coefficient) the value was between [-1, 1] (no information about lag was available).

To avoid having all-to-all connectivity, for PCCWN, LCCWN, PSCWN, LSCWN and PCWN the density was reduced by eliminating 50% of the weakest edges. In case of lag networks (LCCWN and LSCWN), the density reduction was done by considering the corresponding correlation value of the peak in the correlogram (PCCWN / PSCWN) instead of the lag.

On the extracted networks, we applied two different types of network metrics: distance based (APL, BC, CC) and connection based (GCC). In order to allow a comparison between PCCWN, PSCWN and PCWN (peak based networks) we created a set of binary networks by keeping only the strongest 50% of the links. Because we end up with a binary network for the PCWN (if the value is zero, then it is a zero otherwise it is a one), binary networks are considered as well for the PCCWN and PSCWN in order to allow results comparison. In the next section we describe the comparisons between Cross Correlation and Scaled Correlation based networks and Pearson Correlation based networks. In addition to exploring the full 128 node networks, we also grouped the nodes according to the anatomical position of their corresponding electrodes. We used this strategy in order to estimate the interaction between brain areas (occipital, parietal, frontal, temporal) during the visual task. We applied this grouping method only for CCF and SCF based networks (as will be shown, the Pearson network did not offer informative results). Results for each individual area were labeled with a capital letter (e.g Occipital - O, Frontal - F, Left Temporal - LT etc).

5.2 Results

After generating the candidate functional brain networks, we applied the metrics mentioned previously in order to identify how these metrics change from baseline

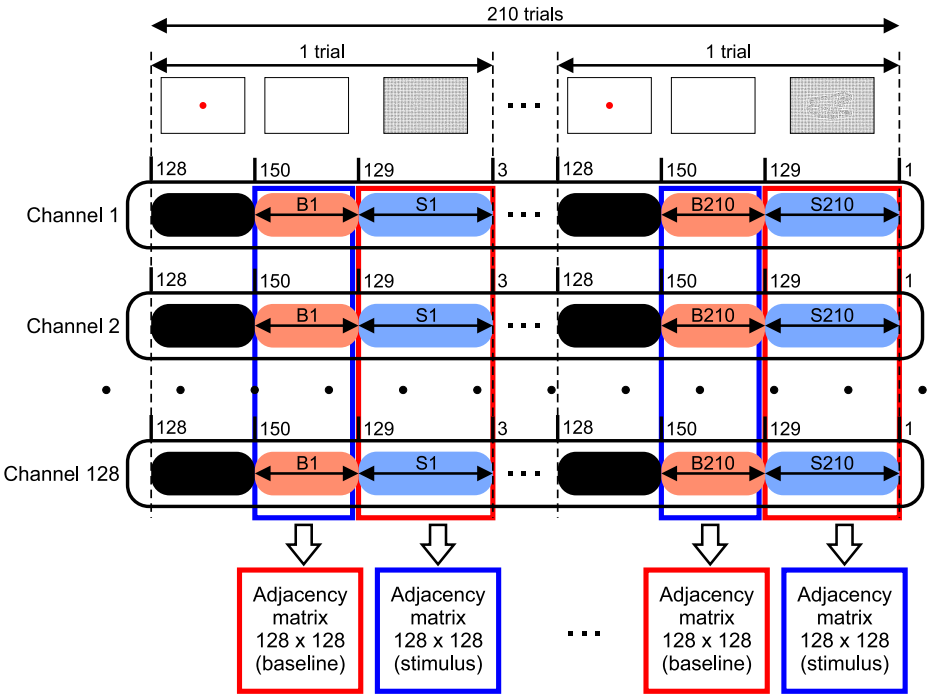

Fig. 2. Schematic representation depicting how the data was extracted from the raw signals. For each participant, 128 signals were recorded as successive trials were presented. A red dot was presented on screen (black segment), followed by a full screen white mask (red segment), after which the stimulus was shown on the screen (blue segment) until the subject pressed a key to signal that i) the stimulus was recognized (code = 1), ii) the subject was uncertain about it (code = 2), iii) the subject saw nothing relevant (code = 3). A 128 x 128 matrix with pairwise correlation values or lags was extracted for each segment corresponding to baseline (B1, B2, ..., B210) and stimulus presentation (S1, S2, ..., S210), yielding a total of 210 matrices associated to baseline and 210 matrices associated to stimulus periods for each subject.

to stimulus periods and as a function of the type of connectivity measure that was used to define the networks.

Fig. 3 (top row) displays the average of APL across the 10 subjects, as a function of the perceptual condition (seen, uncertain, unseen) and depending on the type of network. Clearly, the largest difference between the baseline and stimulus periods is exhibited by LSCWN, indicating a strong reduction in APL when the brain is engaged in perceptual processing. By contrast, neither LCCWN nor PCWN networks showed such a consistent and strong effect.

In Fig. 3 (second row) we show results for GCC, whereby this measure was consistently lower for all networks during the baseline than during the stimulus period. Notably, the largest increase in GCC induced by stimulus presentation was again exhibited by PSCWN, with a close result for PCCWN. Again, PCWN

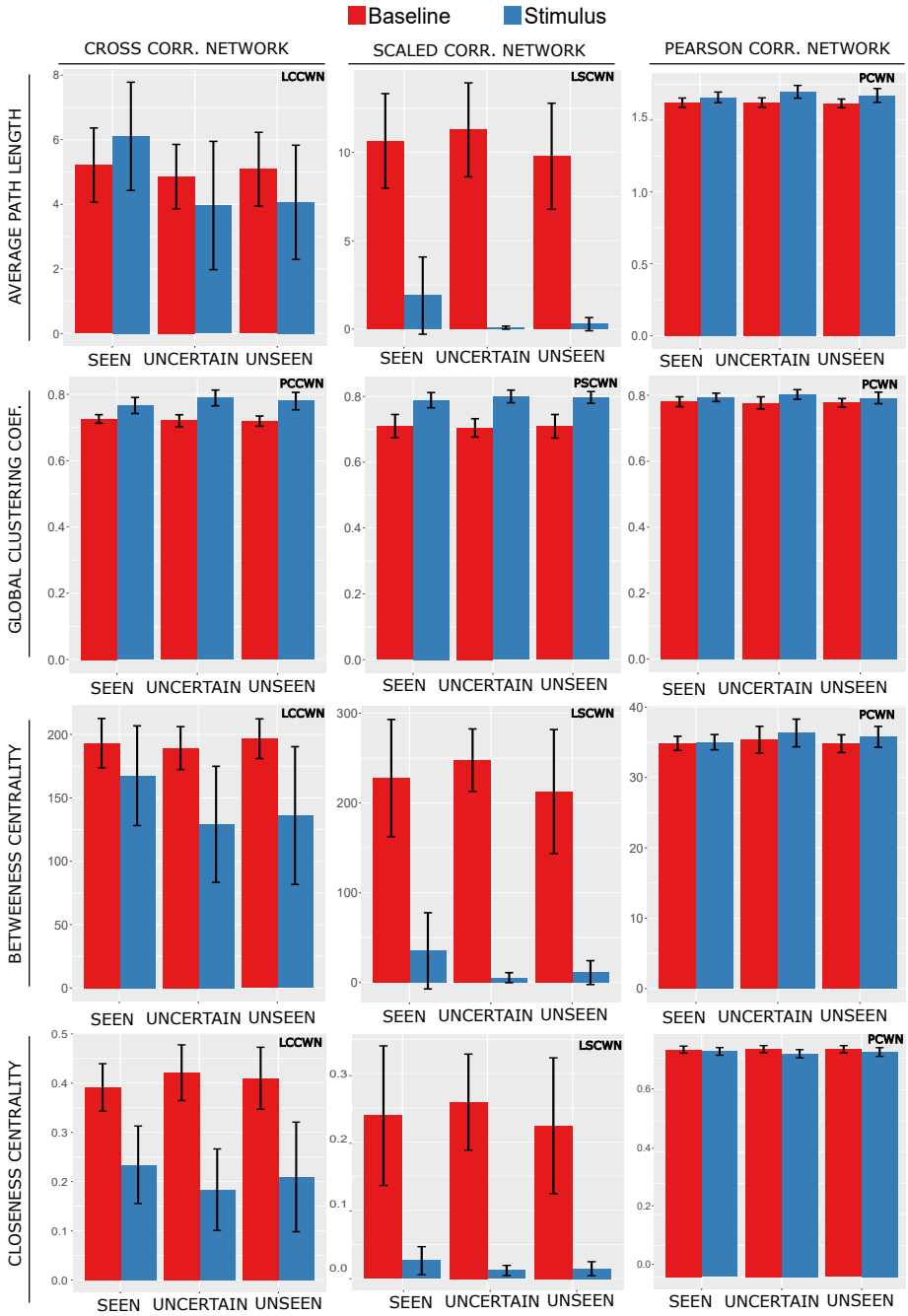

Fig. 3. Metrics applied on our generated networks. APL, BC and CC applied on LCCWN, LSCWN and PCWN. GCC applied on PCCWN, PSCWN and PCWN. For the Scaled Correlation the segment size $s = 25ms$ (fast events - 40Hz). For all networks the density was reduced with 50%. The value obtained is the mean value across all trials and then across all 10 subjects. Error bars are S.D.

performed the worst in terms of showing differences between baseline and stimulus periods.

The BC and CC are illustrated in Fig. 3 (third and fourth rows). As was the case with the other metrics, BC and CC were modulated the strongest for the case of networks extracted with SCF and somewhat less for networks whose definition relied on CCF. Importantly, PCC-based networks did not show a clear modulation of any of the two metrics.

Area level analysis

Since SCF and CCF based networks showed the largest difference between baseline and stimulus, we next focused only on the PCCWN and PSCWN networks. We computed the average across all link weights (average absolute peak correlations). We expected to see higher correlations for the O-F pair when the stimulus was on the screen and a lower correlation in the baseline, because the two areas are actively involved in conscious visual processing. As can be seen in Fig. 4 the PCCWN (Cross Correlation) presents the expected behavior: the correlation between Occipital and Frontal is higher when the stimulus is on the screen meaning that these two areas are better correlated by exchanging more information during the stimulus than during the baseline period. Also was a similarity across all perceptual outcomes (seen, uncertain and unseen) which may indicate that the O-F correlation is non-specific, i.e. it reflects visual processing but no the decision taken by the subject. The effects in the PSCWN (Scaled Correlation) were smaller and this behavior may be the result of considering absolute values of the correlation. For the lags network we expect to see the opposite behavior: a lower lag when the stimulus is shown and a higher lag in the baseline. Fig. 5 shows the mean lags for each pair. The most important thing to notice is the consistency across all perceptual outcomes (seen, uncertain, unseen). Another behavior that can be observed for PCSWN (Scaled Correlation) is the lag being lower (closer to 0) for the stimulus period. This indicates the fact that the overall information may be moving faster during cognitive engagement.

6 Conclusion

We have shown that SCF enables the extraction of functional networks from complex time series in a way that outperforms traditional ones because it can isolate those networks that evolve on particular timescales. As a result, the structure of SCF-extracted networks more readily correlates with the cognitive processes that support visual perception in humans. This is likely due to the fact that fast, gamma oscillations (30-80 Hz) are known to correlate to visual perception, in particular [22], and cognitive processing, in general [23]. SCF is able to estimate the fast interactions between neural populations that occur in the gamma range and reveal the dynamical networks evolving on the fast timescale.

Results also show that PCC-based networks performed the worst in distinguishing the baseline from the stimulus periods. CCF-based networks fared

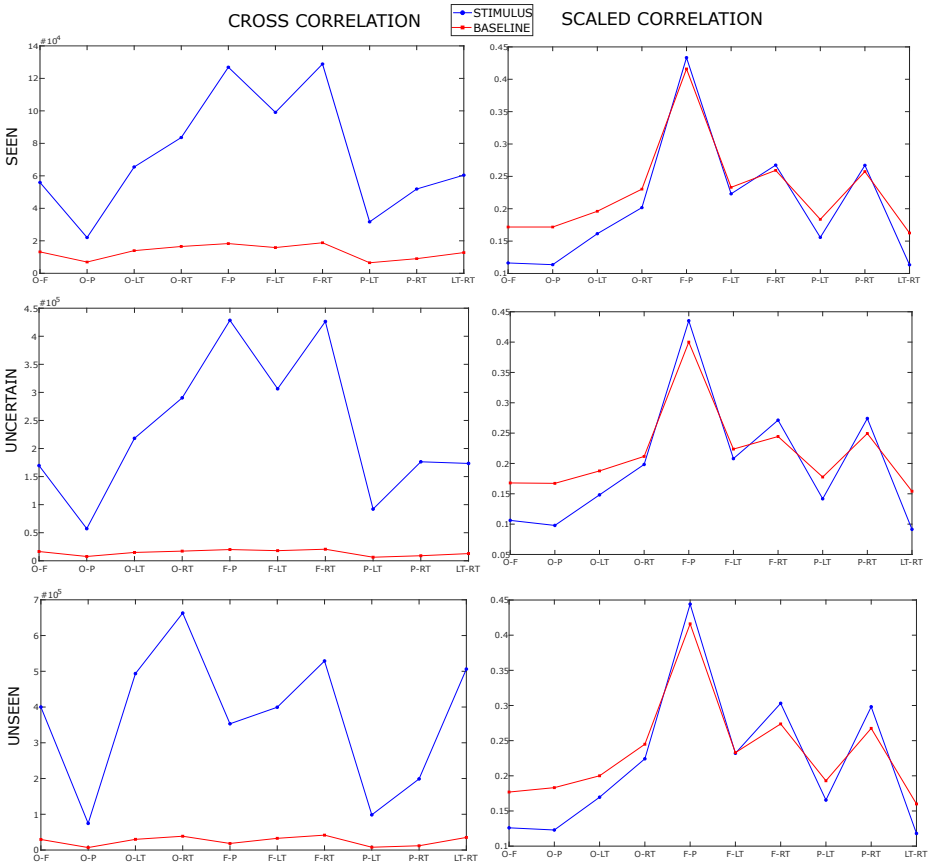

Fig. 4. Areas pairs for PCCWN and PSCWN

better, indicating that information about the temporal relation of signals (delays) is highly relevant in order to properly define the functional brain networks associated to stimulus processing. On top of this temporal information, SCF brings the further advantage that it can select those networks that evolve on the fast timescales, which are known to be co-expressed with perceptual and cognitive processes. The present study suggests that SCF networks may be the preferred choice as they can help define networks that are more likely reflecting the relevant underlying functional brain networks.

The method we have introduced is useful for the investigation of complex brain networks. For example, it could help identify how dynamics of functional networks are altered in brain disorders [24] and may found interesting applications for brain-computer interfaces [25]. However, the applicability of the method is not restricted to neroscience problems. The ability of SCF to extract fast networks from time series opens its applicability range to a wide array of issues where dynamical networks can be found. For example, in climate modeling

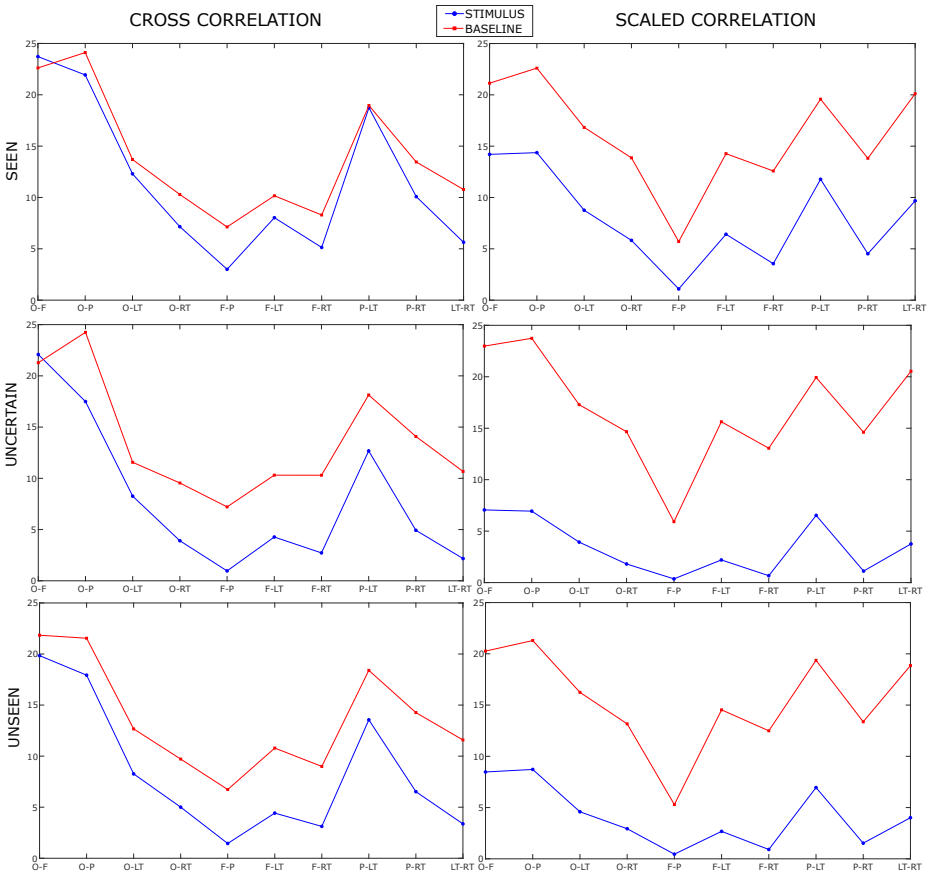

Fig. 5. Areas pairs for LCCWN and LSCWN

thermal disturbances or humidity evolve on various timescales and particular networks may be identified for each. Another example pertains to modeling of coupled chemical processes whose reaction rates may also cover a range of timescales. For all these cases, SCF can enable the selective investigation of dynamical networks that evolve on different timescales. To conclude, the method we have introduced proves very useful for studying brain networks but it is general enough to lend itself to the analysis of dynamical networks from a wide array of research areas.

References

1. Barabasi A.L., Network Science, Cambridge University Press, Jul 21, 2016
2. Marios Koniaris, Ioannis Anagnostopoulos, Yannis Vassiliou, Network Analysis in the Legal Domain: A complex model for European Union legal sources, CoRR, 2015

3. R. Baggio, N. Scott, C. Cooper, Network science: a review focused on tourism, Annals of Tourism Research, 2010
4. E. Bullmore and O. Sporns, Complex brain networks: graph theoretical analysis of structural and functional systems, Nat Rev Neuroscience, vol. 10, no. 4, pp. 312–312, Apr 2009
5. Lange, S., Donges, J. F., Volkholz, J., & Kurths, J. Local Difference Measures between Complex Networks for Dynamical System Model Evaluation. PLoS ONE, 10(4), 2015
6. Karl Pearson, Notes on regression and inheritance in the case of two parents, Proceedings of the Royal Society of London, 58: 240–242, June 20, 1895
7. Bracewell, R., Pentagram Notation for Cross Correlation. The Fourier Transform and Its Applications. New York: McGraw-Hill, pp. 46 and 243, 1965.
8. Nikolić D, Mureşan RC, Feng W, Singer W. Scaled correlation analysis: a better way to compute a cross-correlogram. European Journal of Neuroscience. 35(5):742-62, Mar 1, 2012
9. K. J. Friston, Functional and effective connectivity: A review, Brain Connectivity, vol. 1, no. 1, pp. 13–36, Jan 2011
10. Park HJ, Friston K., Structural and functional brain networks: from connections to cognition. Science. 342(6158):1238411, Nov 1, 2013
11. M. Rubinov and O. Sporns, Complex network measures of brain connectivity: Uses and interpretations, NeuroImage, vol. 52, no. 3, pp. 1059 – 1069, computational Models of the Brain, 2010
12. K. Finc, K. Bonna, M. Lewandowska, T. Wolak, J. Nikadon, J. Dreszer, W. Duch, and S. Khn, Transition of the functional brain network related to increasing cognitive demands, Human Brain Mapping, 2017
13. A. Joudaki, N. Salehi, M. Jalili, and M. G. Knyazeva, EEG based functional brain networks: Does the network size matter?, PLOS ONE, vol. 7, no. 4, pp. 1–9, April 2012
14. M. Jalili and M. G. Knyazeva, Constructing brain functional networks from EEG: partial and unpartial correlations, Journal of integrative neuroscience, vol. 10, no. 2, pp. 213-232, June 2011
15. K. J. Meador and P. G. Ray, Gamma frequency coherence and conscious perception, Journal of Clinical Neurophysiology, vol. 16, no. 2, 1999
16. Bordier, Cécile and Nicolini, Carlo and Bifone, Angelo, Graph Analysis and Modularity of Brain Functional Connectivity Networks: Searching for the Optimal Threshold, Frontiers in Neuroscience, vol. 11, pages. 441, 2017.
17. T. Opsahl, F. Agneessens and J. Skvoretz, Node centrality in weighted networks: Generalizing degree and shortest paths, "Social Networks", vol. 32, no. 3, pp. 245 - 251, Jul 2010
18. A. I. Reppas, K. Spiliotis and C. I. Siettos, Tuning the average path length of complex networks and its influence to the emergent dynamics of the majority-rule model, Mathematics and Computers in Simulation, vol. 109, pp. 186 - 196, March 2015
19. T. Opsahl and P. Panzarasa, Clustering in weighted networks, Social Networks, vol. 31, no. 2, pp. 155 - 163, May 2009
20. Opsahl, T., Agneessens, F., Skvoretz, J., Node centrality in weighted networks: Generalizing degree and shortest paths. Social Networks 32 (3), 245-251, 2010
21. Moca, Vasile V., Ioana Ţincaş, Lucia Melloni, and Raul C. Mureşan. Visual exploration and object recognition by lattice deformation. PloS one 6, no. 7: e22831, 2011

22. Wolf Singer, Neuronal Synchrony: A Versatile Code for the Definition of Relations?, Elsevier (BV), Neuron, September 1999
23. Fries P, Nikolić D, Singer W. The gamma cycle. Trends Neurosci. 30(7):309-16, Jun 6, 2007
24. Stam C.J. Modern network science of neurological disorders. Nature Reviews Neuroscience volume 15, pages 683–695, 2014
25. Jarosiewicz B, Chase SM, Fraser GW, Velliste M, Kass RE, Schwartz AB. Functional network reorganization during learning in a brain-computer interface paradigm. Proc Natl Acad Sci U S A. 105(49):19486-91, Dec 9, 2008